Prospects for measuring coherent neutrino-nucleus elastic scattering at a stopped-pion neutrino source

Kate Scholberg

Department of Physics, Duke University, Durham, North Carolina 27708, USA
(Received 28 November 2005; published 16 February 2006)

Rates of coherent neutrino-nucleus elastic scattering at a high-intensity stopped-pion neutrino source in various detector materials (relevant for novel low-threshold detectors) are calculated. Sensitivity of a coherent neutrino-nucleus elastic scattering experiment to new physics is also explored.

I. INTRODUCTION

Coherent elastic neutral current (NC) neutrino-nucleus scattering [1,2] has never been observed. In this process, a neutrino of any flavor scatters off a nucleus at low momentum transfer Q such that the nucleon wave function amplitudes are in phase and add coherently. The cross section for a spin-zero nucleus, neglecting radiative corrections, is given by [3]

$$\left(\frac{d\sigma}{dE}\right)_{\nu A} = \frac{G_F^2}{2\pi}\frac{Q_w^2}{4}F^2(2ME)M\left[2 - \frac{ME}{k^2}\right], \qquad (1)$$

where k is the incident neutrino energy, E is the nuclear recoil energy, M is the nuclear mass, F is the ground state elastic form factor, Q_w is the weak nuclear charge, and G_F is the Fermi constant. The condition for coherence requires that $Q \lesssim \frac{1}{R}$, where R is the nuclear radius. This condition is largely satisfied for neutrino energies up to ~ 50 MeV for medium A nuclei [2,4].

For neutrino energies up to ~ 50 MeV, typical values of the total coherent elastic cross section are in the range $\sim 10^{-39}$ cm^2, which is relatively high compared to other neutrino interactions in that energy range [e.g. charged current (CC) inverse beta decay on protons has a cross section $\sigma_{\bar{\nu}_e p} \sim 10^{-40}$ cm^2, and elastic neutrino-electron scattering has a cross section $\sigma_{\nu_e e} \sim 10^{-43}$ cm^2].

In spite of its large cross section, coherent elastic neutrino-nucleus scattering has been difficult to observe due to the very small resulting nuclear recoil energies: the maximum recoil energy is $\sim 2k^2/M$, which is in the sub-MeV range for $k \sim 50$ MeV for typical detector materials (carbon, oxygen.) Such energies are below the detection thresholds of most conventional high-mass neutrino detectors. Although there have been suggestions to look for coherent elastic νA scattering of a reactor, spallation source, solar, supernova, or geophysical neutrinos [2,5–7], as yet there has been no successful detection.

However, in recent years there has been a surge of progress in development of novel ultralow threshold detectors, many with the aim of weakly interacting massive particle recoil detection or very low energy solar neutrino detection. Thresholds of 10 keV or even lower for the detection of nuclear recoils may be possible. Such detec-tors include (but are not limited to) noble element (neon, argon, xenon) scintillation, ionization or tracking detectors, solid state detectors (germanium, silicon), bubble and superheated droplet detectors [5,6,8–19]. Some of these new technologies (for instance noble liquid detectors such as CLEAN [8]) may plausibly attain ton-scale masses in the relatively near future.

A promising source of neutrinos for the measurement of coherent elastic cross sections is that arising from a stopped-pion source. Monoenergetic 29.9 MeV ν_μ's are produced from pion decay at rest, $\pi^+ \rightarrow \mu^+ \nu_\mu$, and $\bar{\nu}_\mu$ and ν_e from $\mu^+ \rightarrow \nu_e e^+ \bar{\nu}_\mu$ follow on a muon-decay time scale ($\tau = 2.2$ μs). The neutrino spectral shape is shown in Fig. 1. Neutrinos in this energy range will produce nuclear recoils from coherent scattering with tens of keV. If the beam is pulsed in a short ($< \mu$s) time window, the pion decay ν_μ will be prompt with the beam, and the muon-decay products will be delayed.

Stopped-pion sources of neutrinos have been employed for neutrino experiments in the past [20,21], and future high-flux facilities are planned [22]. The Spallation Neutron Source (SNS) at Oak Ridge National Laboratory should turn on in 2006; J-PARC is another near-term possibility [23]. An experiment to measure neutrino-nucleus CC and NC cross sections (relevant for supernova
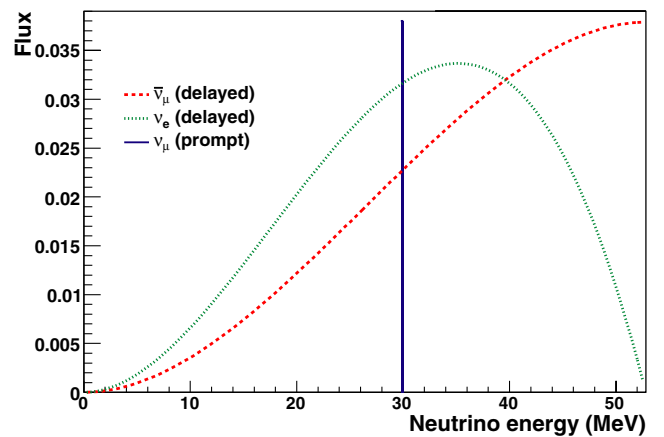

FIG. 1 (color online). Shape of the neutrino spectra from a stopped-pion source, for the different produced flavors.

physics and detection) in the tens of MeV range [24,25] with conventional detectors at the SNS has already been proposed. A shielded concrete bunker is envisioned at a location 20 m from the source; this could potentially accommodate a low-threshold detector as well as the currently planned detectors. The SNS beam is pulsed, with less than microsecond width and a 60 Hz frequency.

Here prospects for measuring coherent elastic neutrino-nucleus scattering will be evaluated using parameters relevant for the SNS; however the results should be generally applicable to experiments at any high-intensity stopped-pion ν source.

II. EXPECTED EVENT RATES

The expected rate of interactions differential in recoil energy is given by

$$\frac{dN}{dE} = N_t \int dk \phi(k) \frac{d\sigma}{dE}(k), \qquad (2)$$

where N_t is the number of targets and $\phi(k)$ is the incident neutrino flux. Spectra for ν_μ, $\bar{\nu}_\mu$ and ν_e for a stopped π^+/μ^+ source, assuming $\sim 10^7 \nu \mathrm{s}^{-1} \mathrm{cm}^{-2}$ per flavor at 20 m from the source are assumed. Cross sections and form factors from [3,26] for ^{20}Ne, ^{40}Ar, ^{76}Ge, and ^{132}Xe are used. Figures 2–5 show the results. The rates are quite promising: for a ton-scale detector with a few to 10 keV threshold, 10^4–10^5 signal events per year are expected.
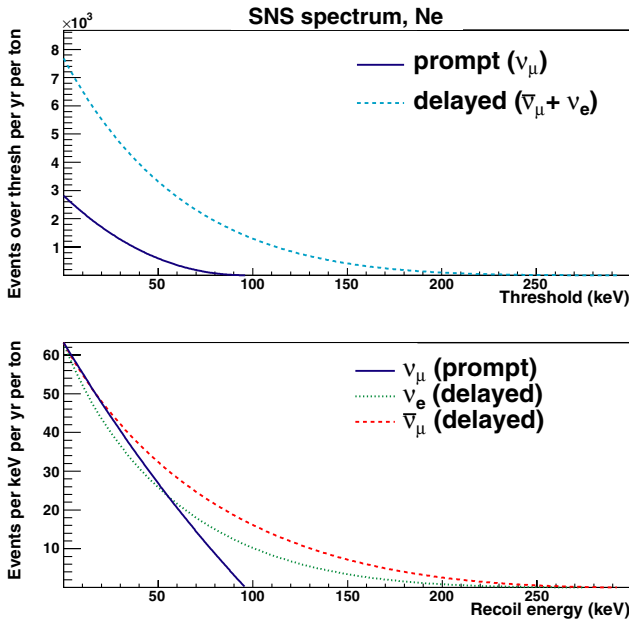

FIG. 3 (color online).   As in Fig. 2 for ^{40}Ar.

Even for kilogram-scale detectors, event rates may be in the tens per year.

Figure 6 plots an integrated yield over threshold for several elements for comparison. One can see that the higher the nuclear mass, the higher the overall event rate at low threshold (scaling approximately as the square of the number of neutrons), but the smaller the typical recoil energies ($E_{\max} = 2k^2/M$).

In the absence of a specific detector model, perfect detection efficiency and zero background are assumed,

FIG. 2 (color online).   Bottom panel: Differential yield at the SNS in 1 ton of ^{20}Ne (solid line: ν_μ, dotted line: ν_e, dashed line: $\bar{\nu}_\mu$) per year per keV, as a function of recoil energy. Top panel: Number of interactions over recoil energy threshold in 1 ton of ^{20}Ne for 1 yr of running at the SNS (solid line: ν_μ, dashed line: sum of ν_e and $\bar{\nu}_\mu$), as a function of the recoil energy threshold.
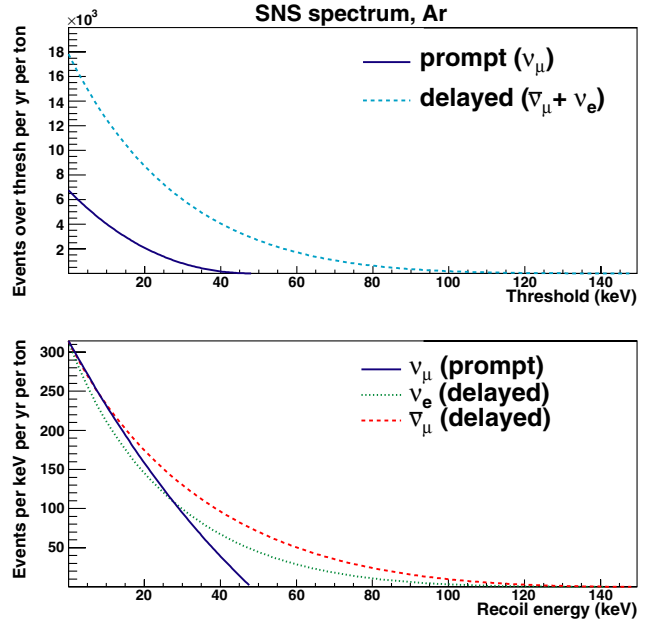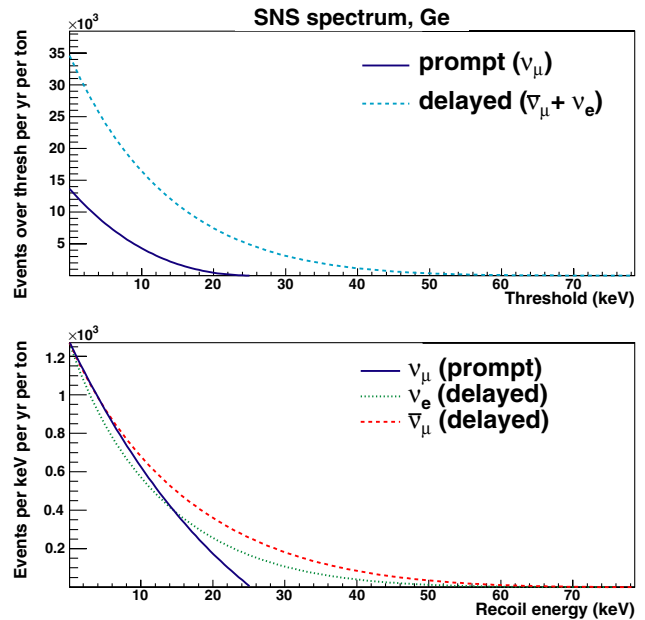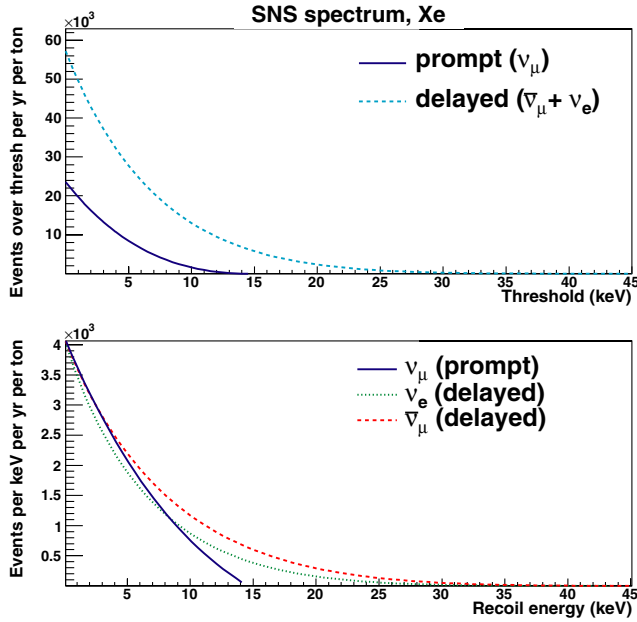

FIG. 4 (color online).   As in Fig. 2 for ^{76}Ge.

FIG. 5 (color online). As in Fig. 2 for ^{132}Xe.

which is not realistic. Detection efficiencies for many low-threshold detector types (see Sec. I) can be reasonably high, but can depend on background levels. Backgrounds will include beam-related neutrons, cosmogenics, radioactivity and instrumental background, as well as other CC and NC neutrino reactions; these will need to be evaluated
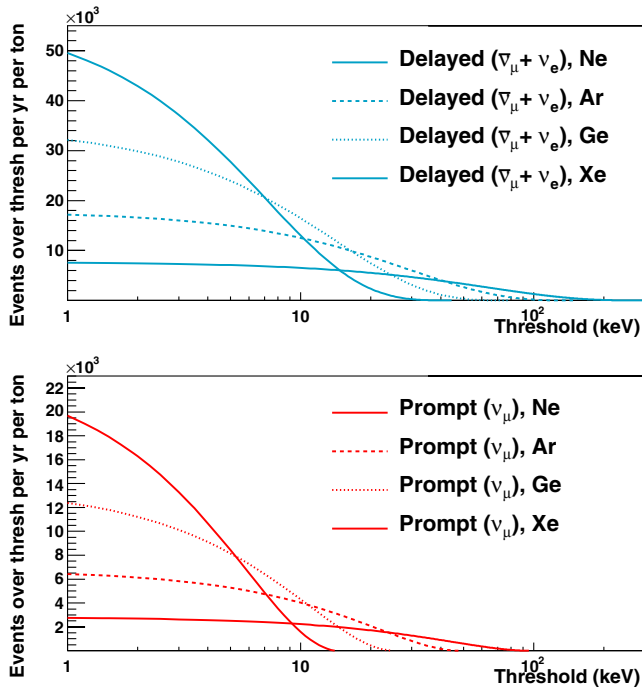
FIG. 6 (color online). The number of interactions over the recoil energy threshold for various detector materials (bottom panel: prompt ν_μ, top panel: sum of delayed ν_e and $\bar{\nu}_\mu$).

for a specific detector's rejection capabilities and location. Backgrounds are not obviously overwhelming, especially given that the pulsed structure of the beam such as that at the SNS leads to a powerful rejection factor ($\sim 4 \times 10^{-4}$) against steady-state backgrounds. It is not really clear at this point whether beam-related backgrounds will be worse for prompt or delayed neutrinos; it will depend on shielding and detector location. Therefore the contributions from prompt and delayed fluxes are given separately.

III. PHYSICS POTENTIAL

The neutrino-nucleus coherent elastic scattering cross section is cleanly predicted by the standard model (SM); form factors can be known to better than 5%, and radiative corrections are known at the percent level [27]. Any measured deviations from prediction would be interesting [28]. In the context of the SM, the weak mixing angle is related to the absolute scattering rate. One can also constrain nonstandard interactions (NSI) of neutrinos and nucleons. Also, a nonzero neutrino magnetic moment will modify the cross section at low energies. There are further reasons to measure coherent neutrino-nucleus scattering: neutrino-nucleus scattering processes are important in supernova physics [1], as well as being useful themselves for supernova neutrino detection [3]. Because they are flavor blind, NC processes allow the measurement of a total neutrino flux, which can be compared to independently measured CC interactions. Therefore one can obtain limits on neutrino oscillation, and, in particular, on oscillations to sterile neutrinos [29]. Finally, it has even been proposed to exploit the large cross sections of neutrino-nucleus scattering for practical neutrino detectors, e.g. reactor monitoring [5,6].

This section will discuss the various ways of probing new physics with a coherent elastic scattering experiment. At this stage, the experimental systematic uncertainty on the absolute rate is not known. It will depend on the specific detector type and configuration, backgrounds, and source uncertainties. However a total systematic uncertainty of ~10% (including nuclear, beam and detector-related uncertainties), while perhaps optimistic, may well be achievable. Systematic uncertainties will likely dominate at the few tens of a kilogram scale or greater.

A. Weak mixing angle

The SM predicts a coherent elastic scattering rate proportional to Q_w^2, the weak charge given by $Q_w = N - (1 - 4\sin^2\theta_W)Z$, where Z is the number of protons, N is the number of neutrons and θ_W is the weak mixing angle. Therefore the weak mixing angle can be extracted from the measured absolute cross section, at a typical Q value of 0.04 GeV/c^2. A deviation from the SM prediction could indicate new physics.

If the absolute cross section can be measured to 10%, there will be an uncertainty on $\sin^2\theta_W$ of ~5%. This is not competitive with the current best measurements from

atomic parity violation [30,31], SLAC E158 [32] and NuTeV [33], which have better than percent-level uncertainties. One would need to significantly improve the systematic uncertainty on the absolute rate (perhaps by normalizing with a well-known rate) for coherent elastic νA scattering in order to make a useful measurement of the weak mixing angle. More promising would be a search for nonstandard interactions of neutrinos with nuclei, as described in the following subsection.

B. Nonstandard interactions of neutrinos

Existing precision measurements of the weak mixing angle at low Q do not constrain new physics which is specific to neutrino-nucleon interactions.

Here a model-independent parametrization of nonstandard contributions to the cross section is used, following Refs. [34,35]. In this description, one assumes an effective Lagrangian for the interaction of a neutrino with a hadron:

$$\mathcal{L}_{\nu H}^{\mathrm{NSI}} = -\frac{G_F}{\sqrt{2}} \sum_{\substack{q=u,d \\ \alpha,\beta=e,\mu,\tau}} [\bar{\nu}_\alpha \gamma^\mu (1-\gamma^5) \nu_\beta](\varepsilon_{\alpha\beta}^{qL}[\bar{q}\gamma_\mu(1-\gamma^5)q]$$
$$+ \varepsilon_{\alpha\beta}^{qR}[\bar{q}\gamma_\mu(1+\gamma^5)q]). \tag{3}$$

The ε parameters describe either "nonuniversal" ($\alpha = \beta$) or flavor-changing ($\alpha \neq \beta$) interactions.

As in Ref. [34], nuclei with total spin zero, and for which the sum of proton spins and the sum of neutron spins is also zero, are considered; in this case we have sensitivity to vector couplings, $\varepsilon_{\alpha\beta}^{qV} = \varepsilon_{\alpha\beta}^{qL} + \varepsilon_{\alpha\beta}^{qR}$. The cross section for coherent NC elastic scattering of neutrinos of flavor α off such a spin-zero nucleus is given by

$$\left(\frac{d\sigma}{dE}\right)_{\nu_\alpha A} = \frac{G_F^2 M}{\pi} F^2 (2ME)\left[1 - \frac{ME}{2k^2}\right]\left\{[Z(g_V^p + 2\varepsilon_{\alpha\alpha}^{uV} + \varepsilon_{\alpha\alpha}^{dV}) + N(g_V^n + \varepsilon_{\alpha\alpha}^{uV} + 2\varepsilon_{\alpha\alpha}^{dV})]^2 + \sum_{\alpha\neq\beta}[Z(2\varepsilon_{\alpha\beta}^{uV} + \varepsilon_{\alpha\beta}^{dV}) + N(\varepsilon_{\alpha\beta}^{uV} + 2\varepsilon_{\alpha\beta}^{dV})]^2\right\}, \tag{4}$$

where Z is the number of protons in the nucleus, N is the number of neutrons, and $g_V^p = (\frac{1}{2} - 2\sin^2\theta_W)$, $g_V^n = -\frac{1}{2}$ are the SM weak constants.

A stopped-pion neutrino source such as that at the SNS contains ν_μ, $\bar{\nu}_\mu$, and ν_e. A coherent elastic νA scattering experiment employing such a source would therefore have sensitivity to all but $\varepsilon_{\tau\tau}$ couplings.

Existing constraints on the values of $\varepsilon_{\alpha\beta}^P$ ($P = L, R$) are summarized in Ref. [35]. Table I selects those relevant for interactions of electron and muon flavor neutrinos with quarks. New constraints from existing and future atmospheric, beam and solar neutrino experiments are explored in Refs. [36,37].

TABLE I. Constraints on NSI parameters, from Ref. [35].

NSI parameter limit	Source
$-1 < \varepsilon_{ee}^{uL} < 0.3$	CHARM $\nu_e N$, $\bar{\nu}_e N$ scattering
$-0.4 < \varepsilon_{ee}^{uR} < 0.7$	
$-0.3 < \varepsilon_{ee}^{dL} < 0.3$	CHARM $\nu_e N$, $\bar{\nu}_e N$ scattering
$-0.6 < \varepsilon_{ee}^{dR} < 0.5$	
$|\varepsilon_{\mu\mu}^{uL}| < 0.003$	NuTeV νN, $\bar{\nu} N$ scattering
$-0.008 < \varepsilon_{\mu\mu}^{uR} < 0.003$	
$|\varepsilon_{\mu\mu}^{dL}| < 0.003$	NuTeV νN, $\bar{\nu} N$ scattering
$-0.008 < \varepsilon_{\mu\mu}^{dR} < 0.015$	
$|\varepsilon_{e\mu}^{uP}| < 7.7 \times 10^{-4}$	$\mu \to e$ conversion on nuclei
$|\varepsilon_{e\mu}^{dP}| < 7.7 \times 10^{-4}$	$\mu \to e$ conversion on nuclei
$|\varepsilon_{e\tau}^{uP}| < 0.5$	CHARM $\nu_e N$, $\bar{\nu}_e N$ scattering
$|\varepsilon_{e\tau}^{dP}| < 0.5$	CHARM $\nu_e N$, $\bar{\nu}_e N$ scattering
$|\varepsilon_{\mu\tau}^{uP}| < 0.05$	NuTeV νN, $\bar{\nu} N$ scattering
$|\varepsilon_{\mu\tau}^{dP}| < 0.05$	NuTeV νN, $\bar{\nu} N$ scattering

From this table, one can see that of these parameters, ε_{ee} and $\varepsilon_{e\tau}$ are quite poorly constrained: values of order unity are allowed. $|\varepsilon_{\mu\beta}|$ couplings are, however, constrained to better than 0.05. Given this situation, the focus here is on ε_{ee} and $\varepsilon_{e\tau}$ couplings [38]. These would be accessible using the electron flavor component of the source. The fact that no oscillations take place (i.e. that the standard three-flavor model of neutrino mixing holds, and that the baseline is too short for significant flavor transition) is also assumed.

The signature of NSI is a deviation from the expected cross section. The following show a few examples of two-dimensional slices of regions in $\varepsilon_{\alpha\beta}$ parameter space that would be allowed if one measured exactly the SM expectation.

Figure 7 shows 90% C.L. allowed regions one would draw for ε_{ee}^{uV}, ε_{ee}^{dV}, if the rate predicted by the SM were measured for the delayed flux (which contains ν_e), assuming that the $\varepsilon_{\mu\beta}$ parameters are negligible, and for $\varepsilon_{e\tau}^{qV} = 0$, for 100 kg/yr of running of a neon detector at 20 m from the source. A 10 keV threshold is assumed. This calculation considers only the total delayed ($\nu_e + \bar{\nu}_\mu$) flux rate [39]. The regions corresponding to assumptions of 5% and 10% systematic error in addition to statistical error, and for statistical error alone are shown [40]. As before, a perfectly efficient, background-free detector is assumed.

Note that in Eq. (4), even in the presence of nonuniversal NSI, one can obtain rates identical to the SM prediction in the case that

$$Z(g_V^p + 2\varepsilon_{ee}^{uV} + \varepsilon_{ee}^{dV}) + N(g_V^n + \varepsilon_{ee}^{uV} + 2\varepsilon_{ee}^{dV})$$
$$= \pm(Zg_V^p + Ng_V^n), \tag{5}$$

so for

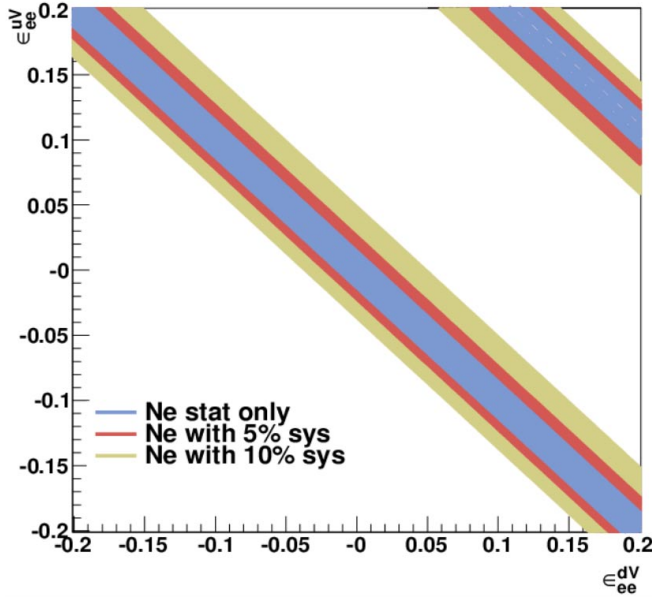$$\varepsilon_{ee}^{uV} = -\frac{(A + N)}{(A + Z)}\varepsilon_{ee}^{dV},$$

FIG. 7 (color online). Allowed region at 90% C.L. for ε_{ee}^{uV} and ε_{ee}^{dV}, for 100 kg/yr of ^{20}Ne at the SNS. The outer region corresponds to an assumed systematic uncertainty of 10% in addition to statistical uncertainty; the middle region corresponds to an assumed systematic uncertainty of 5%, and the inner region corresponds to statistical uncertainty only.

FIG. 8 (color online). Allowed regions at 90% C.L. for ε_{ee}^{uV} and ε_{ee}^{dV}, for 100 /yr each of ^{20}Ne and ^{132}Xe (steeper slope band) at the SNS, assuming 10% systematic uncertainty, plus statistical uncertainty. The thin black ellipses correspond to a combined Ne/Xe measurement. The shaded elliptical region corresponds to a slice of the CHARM experiment's allowed NSI parameter space, for $\varepsilon_{ee}^{qA} = 0$.

and

$$\varepsilon_{ee}^{uV} = -\frac{(A+N)}{(A+Z)}\varepsilon_{ee}^{dV} - \frac{2(Zg_V^p + Ng_V^n)}{A+Z}.$$

For this reason, allowed regions of Fig. 7 appear as linear bands in ε_{ee}^{uV}, ε_{ee}^{dV} parameter space. A measurement employing more than one element can then place more stringent constraints on the couplings; the more the $(A+N)/(A+Z)$ ratio differs between the two targets, the better.

Figure 8 shows the same regions for 100 kg/yr each of ^{132}Xe and ^{20}Ne, where the black ellipses represent the 90% allowed region from the combination of the measurements. These regions are superposed on the allowed region from high-energy ν_e scattering on nucleons derived from CHARM experiment results [41] in Ref. [35], for the case that the axial parameters $\varepsilon_{ee}^{qA} = \varepsilon_{ee}^{qL} - \varepsilon_{ee}^{qR}$ are zero.

Figure 9 shows similar 90% allowed regions for a slice of ε_{ee}^{dV}, $\varepsilon_{e\tau}^{dV}$ parameter space, for $\varepsilon_{ee}^{uV} = \varepsilon_{e\tau}^{uV} = 0$ (note that d-quark NSI may be especially interesting; see e.g. [42]). In this case the allowed parameters correspond to regions between two ellipses. Figure 9 shows regions for a ^{20}Ne detector (with the same assumptions as above). Figure 10 shows the result for ^{132}Xe as well, and the black ellipses contain the region allowed by the combined measurements (for this case, only a small improvement is afforded by measurements with multiple targets).

Figure 11 compares the neutrino-nucleus scattering sensitivity to allowed NSI parameters derived based on a lack
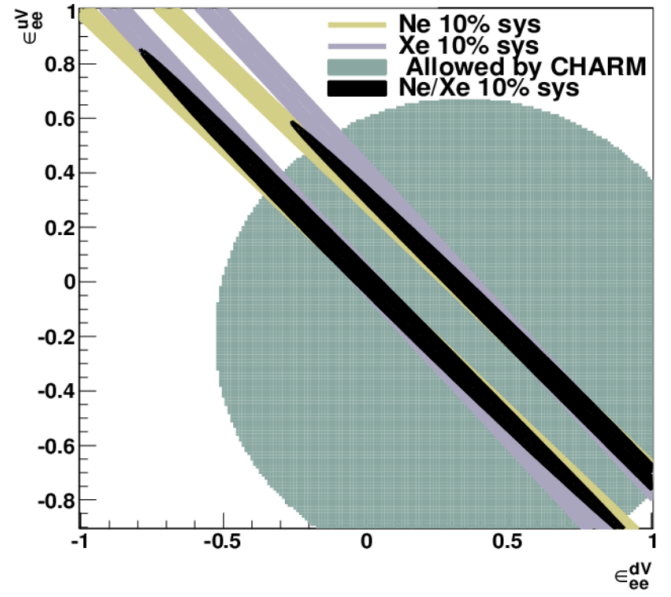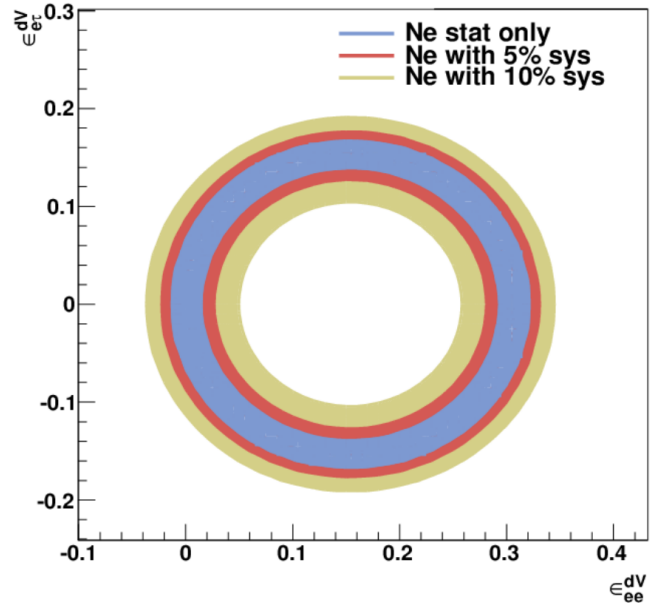

FIG. 9 (color online). Allowed region at 90% C.L. for ε_{ee}^{dV} and $\varepsilon_{e\tau}^{dV}$, for 100 kg/yr of ^{20}Ne at the SNS. The shaded region between the outer and inner ellipses corresponds to an assumed systematic uncertainty of 10% in addition to statistical uncertainty; the next largest region corresponds to an assumed systematic uncertainty of 5%, and the inner region corresponds to statistical uncertainty only.
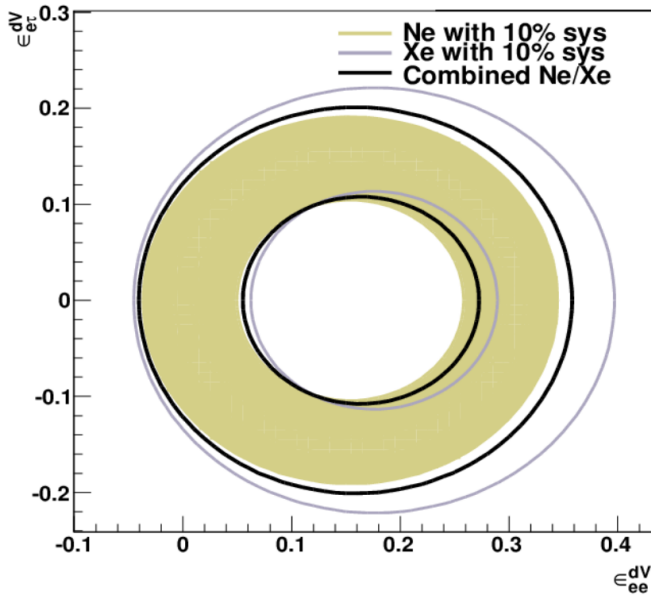
FIG. 10 (color online).   Allowed regions with the same assumptions as Fig. 9, 10% systematic uncertainty for ^{20}Ne (shaded region), ^{132}Xe (region between pale lines) and both combined (region between black lines.)

of distortion of oscillation parameters for beam and atmospheric neutrinos [36].

It is worth noting that a coherent neutrino-nucleus elastic scattering experiment will provide significant con-

straints on still-allowed NSI parameters that modify solar neutrino survival probabilities [37]. As a case in point, consider specific NSI parameters that yield the "LMA-0" solution of Ref. [37]: $\varepsilon_{11}^{uV} = \varepsilon_{11}^{dV} = -0.065$, and $\varepsilon_{12}^{uV} = \varepsilon_{12}^{dV} = -0.15$, where $\varepsilon_{11} = \varepsilon_{ee} - \varepsilon_{\tau\tau} \sin^2\theta_{23}$, and $\varepsilon_{12} = -2\varepsilon_{e\tau} \sin\theta_{23}$, and θ_{23} is the atmospheric mixing angle, known to be $\sim \pi/4$. Following the approach in this reference, $\varepsilon_{\alpha\beta}^{uV} = \varepsilon_{\alpha\beta}^{dV}$ is assumed. Fixing ε_{11} and ε_{12} defined in this way will yield different neutrino-nucleus scattering constraints for different assumptions of $\varepsilon_{\tau\tau}$. Figure 12 shows the value of a χ^2 defined as $\chi^2 = (N_{\mathrm{NSI}} - N_{\mathrm{SM}})^2/\sigma^2$, as a function of $\varepsilon_{\tau\tau}^{uV} = \varepsilon_{\tau\tau}^{dV}$; N_{NSI} is the number of signal events for the given NSI parameters, and N_{SM} is the SM expectation, for 100 kg/yr of ^{20}Ne at the 10 keV threshold; σ^2 includes both statistical uncertainty and an assumed 10% systematic uncertainty. Superimposed on this plot as a shaded region is the restriction on $\varepsilon_{\tau\tau}^{(u,d)V}$ (given assumptions above, and $\varepsilon_{\alpha\beta}^{eV} = 0$) from beam and atmospheric neutrino oscillations, $|1 + \varepsilon_{ee} + \varepsilon_{\tau\tau} - \sqrt{(1 + \varepsilon_{ee} - \varepsilon_{\tau\tau})^2 + 4|\varepsilon_{e\tau}|^2}| < 0.4$, taken from Ref. [36].

From this plot one can see that a coherent elastic neutrino-nucleus scattering experiment has a sensitivity to the set of NSI parameters for which the LMA-0 region is derived. If the rate predicted by the SM were to be observed, these LMA-0 parameters could be ruled out for $\varepsilon_{\tau\tau} = 0$, and would remain viable only for a restricted range of $\varepsilon_{\tau\tau}^{(u,d)V}$.
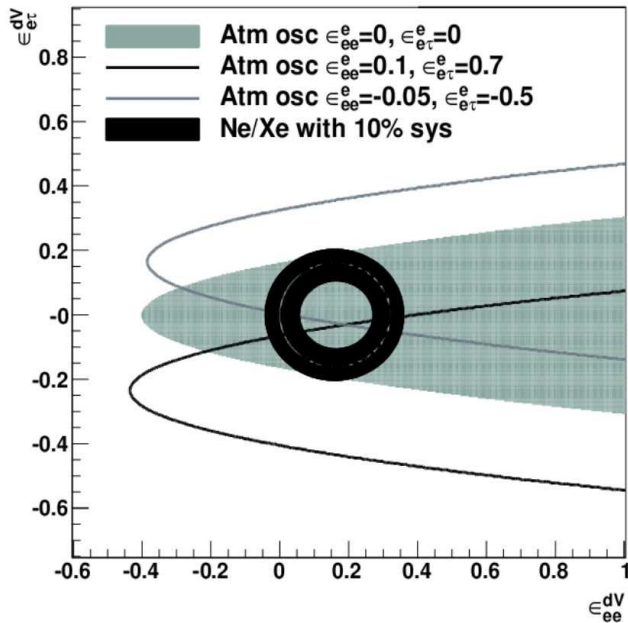

FIG. 11 (color online).   Allowed region at 90% C.L. for ε_{ee}^{dV} and $\varepsilon_{e\tau}^{dV}$, $\varepsilon_{ee}^{uV} = \varepsilon_{e\tau}^{uV} = 0$, for 100 kg/yr each of ^{20}Ne and ^{132}Xe at the SNS is shown in black. The shaded region corresponds to a slice of allowed NSI parameters from Ref. [36] for $\varepsilon_{\tau\tau} = 0$, and $\varepsilon_{ee}^{eV} = \varepsilon_{e\tau}^{eV} = 0$; the parabolic regions inside the dark and light lines correspond to slices of allowed parameter space for some specific values of ε_{ee}^{eV} and $\varepsilon_{e\tau}^{eV}$.
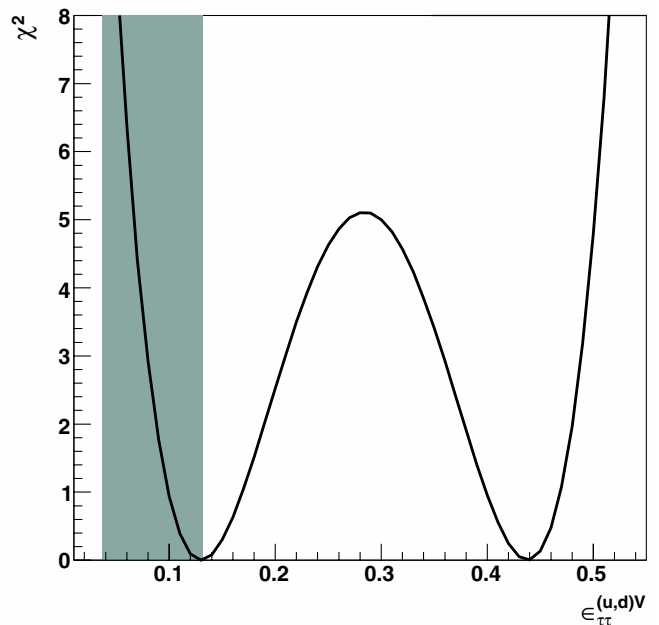

FIG. 12 (color online). χ^2 as a function of $\varepsilon_{\tau\tau}^{(u,d)V}$ for 100 kg/yr of a ^{20}Ne, assuming NSI parameters $\varepsilon_{11}^{(u,d)V} = -0.065$ and $\varepsilon_{12}^{(u,d)V} = -0.15$. The shaded region represents allowed $\varepsilon_{\tau\tau}$ parameters from Ref. [36], from beam and atmospheric neutrino oscillation constraints.

The conclusion of these NSI studies is that a coherent elastic neutrino-nucleus scattering experiment at a stopped-pion source would have significant sensitivity to currently allowed NSI ε_{ee}^{qV} and $\varepsilon_{e\tau}^{qV}$ parameters.

C. Neutrino magnetic moment

The SM predicts a neutrino magnetic moment of $\mu_\nu \lesssim 10^{-19} \mu_B (m_\nu/1 \text{ eV})$, in units of Bohr magnetons. This is very small, but extensions of the SM commonly predict larger ones. The most stringent limits are astrophysical: for instance, based on a lack of observed energy loss from electromagnetic couplings in a red giant evolution one can set a limit $\mu_\nu \lesssim 10^{-12} \mu_B$ [43]. The best direct experimental limits result from a lack of distortion of neutrino-electron elastic scattering at low energy, and are in the range of $\mu_\nu(\nu_e) \lesssim 1\text{–}2 \times 10^{-10} \mu_B$ [44–46]. For muon neutrino scattering, the best limit is less stringent: $\mu_\nu(\nu_\mu) \lesssim 6.8 \times 10^{-10} \mu_B$ [47].

A signature of nonzero neutrino magnetic moment can be observed via distortion of the recoil spectrum of coherently scattered nuclei. The magnetic scattering cross section is given in Ref. [48] for a spin-zero nucleus:

$$\left(\frac{d\sigma}{dE}\right)_m = \frac{\pi \alpha^2 \mu_\nu^2 Z^2}{m_e^2}\left(\frac{1 - E/k}{E} + \frac{E}{4k^2}\right). \quad (6)$$

Figure 13 shows the differential cross sections calculated for ^{20}Ne, for 30 MeV neutrino energy, as a function of nuclear recoil energy. The magnetic scattering cross section is calculated for the neutrino magnetic moment just below the current best experimental limits ($10^{-10} \mu_B$ for ν_e and $6 \times 10^{-10} \mu_B$ for ν_μ).
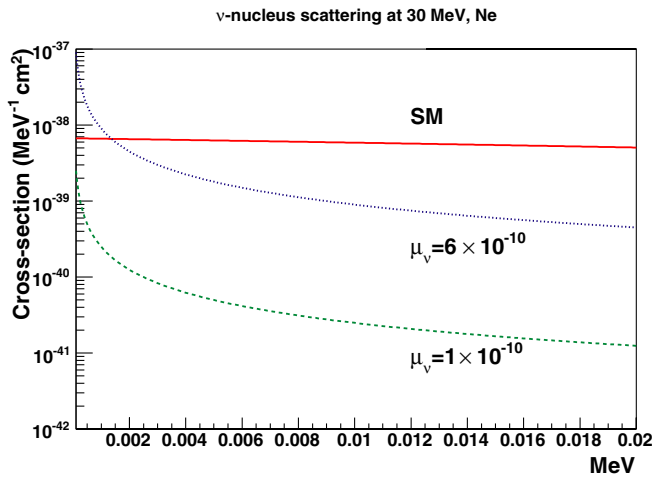

ν-nucleus scattering at 30 MeV, Ne

FIG. 13 (color online). Solid line: SM coherent neutrino-nucleus differential cross section, as a function of nuclear recoil energy E, for neutrino energy $k = 30$ MeV and for a ^{20}Ne target. Dashed line: differential cross section for neutrino-nucleus scattering due to a neutrino magnetic moment of $\mu_\nu = 10^{-10} \mu_B$. Dotted line: differential cross section for neutrino-nucleus scattering due to a neutrino magnetic moment of $\mu_\nu = 6 \times 10^{-10} \mu_B$.

Figure 14 shows the yield in events per keV of recoil energy, per ton per year in a neon detector at 20 m from the SNS target, with and without a neutrino magnetic moment contribution, for prompt and delayed fluxes. The dashed lines assume $\nu_\mu = 10^{-10} \mu_B$ for both ν_e and $\bar{\nu}_\mu$. The dotted lines assume $\nu_\mu = 10^{-10} \mu_B$ for ν_e and $\nu_\mu = 6 \times 10^{-10} \mu_B$ for $\bar{\nu}_\mu$.

The difference in the coherent neutrino-nucleus scattering yield due to the presence of a neutrino magnetic moment near the current μ_ν limit for ν_e is very small, except for recoil energies below a few keV. This signal is therefore likely out of reach for a CLEAN-type experiment at the SNS. However, for μ_ν near the current limit for ν_μ, there might be a measurable signal for a 10 keV threshold, and it is conceivable that one could improve the limit with a high-statistics measurement. Nuclei with spin, although not considered here, have additional μ_ν-dependent terms in their coherent neutrino-nucleus scattering cross sections [48] and may be potential targets for a neutrino magnetic moment search [49].

IV. CONCLUSION

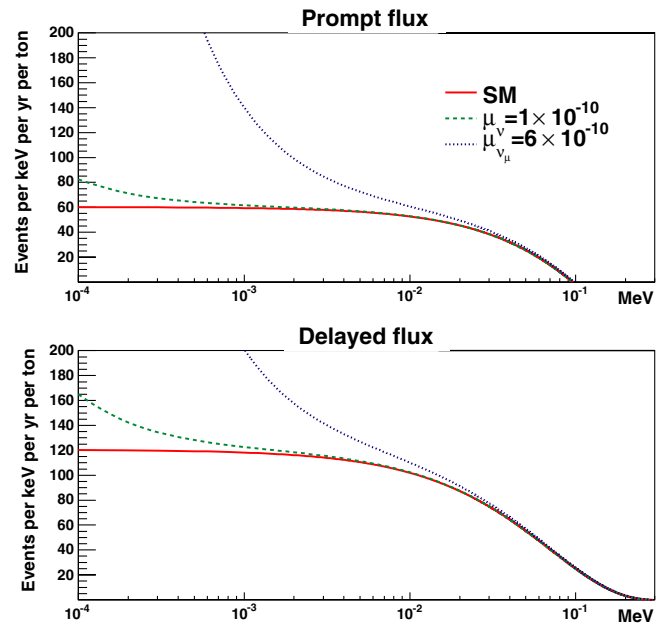Straightforward calculations indicate that one expects thousands of coherent neutrino-nucleus interactions with

FIG. 14 (color online). Differential yield at the SNS in neon as a function of nuclear recoil energy. The top plot is for the prompt flux (ν_μ only) and the bottom plot is for the delayed flux (sum of ν_e and $\bar{\nu}_\mu$). Solid lines: SM expectation. Dashed lines: yield including magnetic moment contribution for $\mu_\nu = 10^{-10} \mu_B$ for both ν_e and $\bar{\nu}_\mu$. Dotted lines: yield including magnetic moment contribution for $\mu_\nu = 10^{-10} \mu_B$ for ν_e and $\mu_\nu = 6 \times 10^{-10} \mu_B$ for $\bar{\nu}_\mu$, ν_μ.

recoil energies >10 keV per ton of material per year of running at the SNS, which is very promising. Even few kilogram-scale experiments may have measurable rates. These estimates have been made for an experiment with no background and no inefficiency; both will certainly be important for a real experiment. Sensitivities will need to be reevaluated for a specific detector configuration for which backgrounds and efficiencies can be estimated.

Unambiguous detection of the process is a first step; high-statistics measurements will then follow. Such an experiment has significant potential for constraining NSI parameters; magnetic moment and precision weak mixing angle measurements are also conceivable, although they pose a greater experimental challenge.

[1] D. Z. Freedman, D. N. Schramm, and D. L. Tubbs, Annu. Rev. Nucl. Sci. **27**, 167 (1977).
[2] A. Drukier and L. Stodolsky, Phys. Rev. D **30**, 2295 (1984).
[3] C. J. Horowitz, K. J. Coakley, and D. N. McKinsey, Phys. Rev. D **68**, 023005 (2003).
[4] F. Boehm and P. Vogel, *Physics of Massive Neutrinos* (Cambridge University Press, Cambridge, 1987).
[5] P. Barbeau, J. I. Collar, J. Miyamoto, and I. Shipsey, IEEE Trans. Nucl. Sci. **50**, 1285 (2003).
[6] C. Hagmann and A. Bernstein, IEEE Trans. Nucl. Sci. **51**, 2151 (2004).
[7] H. T. Wong, hep-ex/0511001.
[8] D. N. McKinsey and K. J. Coakley, Astropart. Phys. **22**, 355 (2005).
[9] M. G. Boulay, A. Hime, and J. Lidgard, nucl-ex/0410025.
[10] M. G. Boulay and A. Hime, astro-ph/0411358.
[11] E. Aprile *et al.*, Phys. Rev. D **72**, 072006 (2005).
[12] Y. Takeuchi, in *Proceedings of the 32nd International Conference on High-Energy Physics (ICHEP 04), Beijing, China, 2004* (World Scientific, Hackensack, 2004).
[13] G. J. Alner *et al.* (UK Dark Matter Collaboration), Astropart. Phys. **23**, 444 (2005).
[14] D. P. Snowden-Ifft, T. Lawson, N. J. C. Spooner, and N. Villaume, Nucl. Instrum. Methods Phys. Res., Sect. A **516**, 406 (2004).
[15] R. Galea, http://snolab2005.snolab.ca/talks/Snolab_workshopIV_galea_ebubble.pdf
[16] D. S. Akerib *et al.*, Nucl. Instrum. Methods Phys. Res., Sect. A **520**, 163 (2004).
[17] D. S. Akerib *et al.*, Nucl. Instrum. Methods Phys. Res., Sect. A **520**, 116 (2004).
[18] W. J. Bolte *et al.*, astro-ph/0503398.
[19] M. Barnabe-Heider *et al.* (PICASSO Collaboration), Nucl. Instrum. Methods Phys. Res., Sect. A **555**, 184 (2005).
[20] C. Athanassopoulos *et al.* (LSND Collaboration), Nucl. Instrum. Methods Phys. Res., Sect. A **388**, 149 (1997).
[21] R. L. Burman, Nucl. Instrum. Methods Phys. Res., Sect. A

368, 416 (1996).
[22] I. S. K. Gardner, in *Proceedings of the 6th European Particle Accelerator Conference (EPAC 98), Stockholm, Sweden, 1998* (IOP Publishing, Philadelphia, 1998).
[23] Y. Ikeda, http://www.fz-juelich.de/ess/datapool/icanspdf/Ikeda-G3-paper.pdf
[24] F. T. Avignone and Y. V. Efremenko, J. Phys. G **29**, 2615 (2003).
[25] Nu-SNS Collaboration, http://www.phy.ornl.gov/nusns/proposal.pdf
[26] C. J. Horowitz and G. Shen (private communication).
[27] C. J. Horowitz (private communication).
[28] L. M. Krauss, Phys. Lett. B **269**, 407 (1991).
[29] Note that for an SNS configuration, most sterile oscillation scenarios are already quite well constrained by other experiments, especially assuming a null result from mini-BooNE.
[30] S. C. Bennett and C. E. Wieman, Phys. Rev. Lett. **82**, 2484 (1999).
[31] S. Eidelman *et al.* (Particle Data Group Collaboration), Phys. Lett. B **592**, 1 (2004).
[32] P. L. Anthony *et al.* (SLAC E158 Collaboration), Phys. Rev. Lett. **95**, 081601 (2005).
[33] G. P. Zeller *et al.* (NuTeV Collaboration), Phys. Rev. Lett. **88**, 091802 (2002); **90**, 239902 (2003).
[34] J. Barranco, O. G. Miranda, and T. I. Rashba, J. High Energy Phys. 12 (2005) 021.
[35] S. Davidson, C. Peña Garay, N. Rius, and A. Santamaria, J. High Energy Phys. 03 (2003) 011.
[36] A. Friedland and C. Lunardini, Phys. Rev. D **72**, 053009 (2005).
[37] A. Friedland, C. Lunardini, and C. Peña Garay, Phys. Lett. B **594**, 347 (2004).
[38] One might conceivably eventually confront the current best $\varepsilon_{\mu\tau}$ limits with an SNS coherent elastic scattering experiment.
[39] In principle one might do better with a spectral fit to separate ν_μ and $\bar{\nu}_e$ contributions.
[40] Note that one might achieve some cancellation of absolute

source-flux-related systematic uncertainty by taking a ratio of prompt and delayed fluxes.

[41] J. Dorenbosch *et al.* (CHARM Collaboration), Phys. Lett. B **180**, 303 (1986).

[42] P. S. Amanik, G. M. Fuller, and B. Grinstein, Astropart. Phys. **24**, 160 (2005).

[43] G. G. Raffelt, Phys. Rep. **320**, 319 (1999).

[44] D. W. Liu *et al.* (Super-Kamiokande Collaboration), Phys. Rev. Lett. **93**, 021802 (2004).

[45] Z. Daraktchieva *et al.* (MUNU Collaboration), Phys. Lett. B **615**, 153 (2005).

[46] H. T. Wong, Nucl. Phys. B, Proc. Suppl. **143**, 205 (2005).

[47] L. B. Auerbach *et al.* (LSND Collaboration), Phys. Rev. D **63**, 112001 (2001).

[48] P. Vogel and J. Engel, Phys. Rev. D **39**, 3378 (1989).

[49] Note that a neutrino-electron magnetic scattering search can in principle be done at the SNS with low-threshold detectors. The νe magnetic scattering cross section is smaller by a factor of Z^2 than for the neutrino nucleus, but there is a factor of Z more electron targets, so the signal is overall a factor of 10 smaller than for νA. This amounts to $\sim 10 \nu e$ magnetic scattering events per ton per year at the SNS above 10 keV, for μ_ν at the current ν_μ limit. The νe magnetic signal has negligible SM background; however absolute rates are low for realistic target masses and likely to be subject to experimental backgrounds.